

## Article

# Measurement of Gaseous Exhaust Emissions of Light-Duty Vehicles in Preparation for Euro 7: A Comparison of Portable and Laboratory Instrumentation

Victor Valverde <sup>1</sup>, Yosuke Kondo <sup>2</sup>, Yoshinori Otsuki <sup>2</sup>, Torsten Krenz <sup>3</sup>, Anastasios Melas <sup>1</sup>, Ricardo Suarez-Bertoa <sup>1</sup> and Barouch Giechaskiel <sup>1,\*</sup>

<sup>1</sup> European Commission, Joint Research Centre (JRC), 21027 Ispra, Italy

<sup>2</sup> HORIBA Ltd., Shiga 520-0102, Japan

<sup>3</sup> HORIBA Europe GmbH, 42799 Leichlingen, Germany

\* Correspondence: barouch.giechaskiel@ec.europa.eu; Tel.: +39-0332-78-5312

**Abstract:** The European Union's ambition to reach climate neutrality and a toxic-free environment by 2050 entails, among other things, cleaner road vehicles. The European Commission's proposal for the next regulatory emissions standard, Euro 7, requires the measurement of pollutants currently not regulated on the road. In this study we compared a prototype portable emissions measurement system (PEMS) measuring CO<sub>2</sub>, CO, NO, NO<sub>2</sub>, N<sub>2</sub>O, NH<sub>3</sub>, CH<sub>4</sub>, and HCHO based on infrared laser absorption modulation (IRLAM), and two Fourier transform infrared (FTIR) spectrometers with laboratory grade analyzers. To this end, one Euro 6d Diesel, one Euro 6d gasoline, and one Euro 4 gasoline vehicle were tested at −7 °C and 23 °C with various driving cycles covering traffic conditions to highway dynamic driving. The results demonstrated that the differences among the instruments were small: ±1 mg/km for HCHO, N<sub>2</sub>O, and CH<sub>4</sub>, ±2.5 mg/km for NH<sub>3</sub>, ±10–15 mg/km for NO<sub>x</sub>, ±50 mg/km or ±15% for CO (whichever was larger), and ±10–15 g/km for CO<sub>2</sub>. These values corresponded to <10–15% of the proposed Euro 7 limits or the emission levels of the tested vehicles. Our results confirm the feasibility of on-board systems to measure the conventional components including CO<sub>2</sub> and the aforementioned additional pollutants.

**Keywords:** Euro 7; vehicle emissions; ammonia; N<sub>2</sub>O; PEMS; FTIR; IRLAM



**Citation:** Valverde, V.; Kondo, Y.; Otsuki, Y.; Krenz, T.; Melas, A.; Suarez-Bertoa, R.; Giechaskiel, B. Measurement of Gaseous Exhaust Emissions of Light-Duty Vehicles in Preparation for Euro 7: A Comparison of Portable and Laboratory Instrumentation. *Energies* **2023**, *16*, 2561. <https://doi.org/10.3390/en16062561>

Academic Editor: Mejdi Jeguirim

Received: 31 January 2023

Revised: 6 March 2023

Accepted: 7 March 2023

Published: 8 March 2023



**Copyright:** © 2023 by the authors. Licensee MDPI, Basel, Switzerland. This article is an open access article distributed under the terms and conditions of the Creative Commons Attribution (CC BY) license (<https://creativecommons.org/licenses/by/4.0/>).

## 1. Introduction

In the European Union (EU), the human exposure to concentrations of fine particulate matter (PM) and nitrogen dioxide (NO<sub>2</sub>) above the World Health Organization (WHO) guideline levels caused respectively 238,000 and 49,000 premature deaths, in 2020 [1]. Considering that the number of deaths for all causes in the EU in 2020 was 5.18 million [2], fine PM and NO<sub>2</sub> air pollution was responsible for circa 4.6% and 1% of all deaths, respectively. In the same period, road transport contributed to 9% of fine PM and 37% of nitrogen oxides (NO<sub>x</sub>) emissions in the EU [1]. Vehicle emission standards have been developed to limit the emissions of a number of pollutants found in the vehicles' exhaust as result of combustion of fossil fuels. They were first introduced in the EU in 1977 for light-duty (LD) vehicles with Directive 77/102/EEC and in 1988 for heavy-duty (HD) engines with Directive 88/77/EEC [3,4]. Since then, the emission standards have constantly evolved towards more restrictive limits and using more representative test procedures that cover more realistic conditions. As a consequence of the enforcement of emissions regulations in the EU, in 2020 fine PM and NO<sub>x</sub> emissions from road transport were 60.8% and 65.7% lower than in 1990, respectively [5]. In order to strengthen the vehicle emissions regulations, To this end, the latest LD and HD standards (Euro 6 and Euro VI, respectively) introduced the use of portable emissions measurement systems (PEMS) that allowed moving from the laboratory environment to more representative on-road conditions (Regulation 2017/1151

for LD, Regulation 582/2011 for HD). These on-road tests are known as real-driving emissions (RDE) tests for LD and PEMS tests for the HD counter parts. The tests are driven on public roads under real traffic and meteorological conditions without a predefined speed profile (additional details on the PEMS tests for LD and HD can be checked elsewhere [6,7]). Euro 6 RDE test procedures prescribe the measurement of  $\text{NO}_x$ , solid particle number with a cut-off size of 23 nm, carbon monoxide (CO) and carbon dioxide ( $\text{CO}_2$ ), although emission limits are applicable only for  $\text{NO}_x$  and particles (particles are not applicable for port-fuel injected light-duty spark ignition vehicles). On the other hand, Euro VI HD PEMS testing requires the measurement of particles, CO, total hydrocarbons (THC), methane ( $\text{CH}_4$ ),  $\text{NO}_x$ , and  $\text{CO}_2$ . The measurement of these pollutants in a real world operation needs to address the intrinsic differences between the laboratory and the on-road procedures. Differences include, but are not limited to: static measurement from a bag in the laboratory vs. dynamic measurement from the tailpipe during the on-road test, or the much longer measurement periods of the on-road tests (~3 times) when compared to the laboratory tests that could lead to instrumental drifts. To cope with these measurement principle methodological differences, the so-called conformity factors were introduced for both LD and HD in Euro 6/VI. The conformity factors reflect the additional PEMS uncertainty as compared to the laboratory measurement [8].

The EU has set a high ambition level to reach climate neutrality by 2050, as well as a zero-pollution ambition for a toxic-free environment, that require cleaner road vehicles entering the market. Some of the pollutants, currently not regulated, have adverse health and environmental impacts. For example, formaldehyde (HCHO) is classified as a human carcinogen (Group 1) by the International Agency for Research on Cancer (IARC), and is a reactive contributing to atmospheric photochemistry [9]. Non-methane organic gases (NMOG) contribute to the formation of the ground-level ozone, which causes adverse health effects, damages plants and infrastructures, and increases global warming [10]. Based on the Intergovernmental Panel on Climate Change (IPCC),  $\text{N}_2\text{O}$  is a strong greenhouse gas with a Global Warming Potential (GWP) of 265 on a 100-year basis, and it also depletes stratospheric ozone. Ammonia ( $\text{NH}_3$ ) is a toxic and corrosive gas, and it is a precursor of secondary aerosols and smog causing adverse health, climate, and visibility impairment effects [11].

The European Commission recently proposed the latest vehicle emissions Regulation, Euro 7 [12]. This new standard reexamined the emission limits for LD and HD and requires the measurement of additional pollutants on-road and in laboratory conditions over a wide range of ambient conditions. For LD vehicles, in addition to the currently Euro 6 regulated  $\text{NO}_x$ , the following gaseous pollutants have to be measured on the road: CO, THC, non-methane hydrocarbons (NMHC), and  $\text{NH}_3$ . NMHC are determined from THC and  $\text{CH}_4$  measurements. For HD vehicles, in addition to  $\text{NO}_x$ , CO, and  $\text{CH}_4$ , which are currently regulated with Euro VI, NMOG, HCHO,  $\text{N}_2\text{O}$ , and  $\text{NH}_3$  have to be measured. Note that  $\text{NH}_3$  was required for laboratory Euro VI measurements but not for on-road testing. According to the proposal, the Euro 7 emission limits have been set taking into account the measurement uncertainty of the instruments, and hence no conformity factors are foreseen in Euro 7 (i.e., PEMS measurement uncertainty is included in the emission limits). The new Euro 7 standard has been proposed to enter into force in 2025 for LD vehicles and 2027 for HD vehicles. The Euro 7 emission standard is meant to secure low pollutants emissions from new vehicles in Europe in the transition period until full adoption of a zero-tailpipe emissions fleet.

As a consequence of the enforcement of regulatory requirements, aftertreatment devices have improved [13–16]. The measurement technologies are also evolving and new technologies are being suggested to measure the new pollutants during real world operation [17–20]. HORIBA has developed a prototype PEMS in view of the upcoming Euro 7 emission standard using the quantum cascade laser infrared (QCL-IR) principle and measures eight components that will be regulated under the Euro 7 standard. Previous studies with previous versions of the instrument, but with fewer components, were promis-

ing [21,22]. In Euro 6/VI regulation specific measurement principles are prescribed for the measurement of the gaseous compounds (i.e., these are considered to be the “standard” analyzers). For example, only non-dispersive infrared detectors is permitted for CO. QCL-IR and Fourier-transform infrared (FTIR) technologies are not included. Equivalence for “alternative” techniques can be demonstrated by laboratory and on-road testing comparing with the “standard” techniques. The documentation supporting such demonstration needs a description of the theoretical basis, testing covering vibrations, ambient and altitude boundaries of the RDE conditions, and comparisons with “standard” and/or laboratory grade analyzers for both gasoline and diesel engines.

The aim of the campaign organized by the European Commission Joint Research Center (JRC) in collaboration with HORIBA was to investigate the performance of the prototype QCL-IR-based PEMS and two FTIRs in laboratory conditions on different vehicles under a wide range of testing conditions. Based on the comparisons of “standard” and “alternative” techniques quantitative differences between the instruments is provided for conventional pollutants and the pollutants now included in the Euro 7. Particular attention is given to the lower range, where future vehicle technologies are expected to emit. The findings of this study will provide support in defining the permissible principles for the measurement of various pollutants in the upcoming Euro 7 regulation.

## 2. Materials and Methods

This section describes the experimental setup, the characteristics of the prototype PEMS and the laboratory-grade instruments used, the tested vehicles, as well as the test cycles that were driven.

### 2.1. Setup

The experimental campaign was carried out in the JRC’s vehicle emissions laboratory (VELA 2) in the second half of October 2022. No on-road tests were performed with the prototype PEMS, because the scope of the campaign was to assess the performance of the instrument on a wide range of ambient conditions, and on a number of vehicles with different exhaust characteristics. VELA 2 consists of a two-axle chassis dynamometer in a climatic chamber with controlled ambient temperature and humidity. The laboratory is equipped with a full dilution tunnel with constant volume sampling (CVS) and critical flow Venturi to measure total air flow and a smooth-approach orifice (SAO) to measure dilution air flow. The exhaust gas emissions were measured directly at the tailpipe by four different instruments (Figure 1), and in the dilution tunnel by the laboratory gas analyzers. Part of the diluted gas was also collected in Tedlar bags and analyzed following the regulatory requirements for the type 1 test as described in Regulation (EU) 2017/1151. The technical details of all instruments are provided in the following sections.

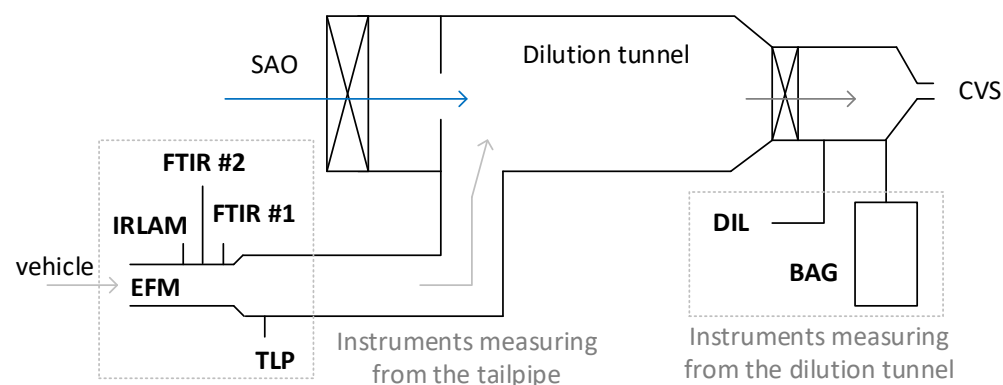


**Figure 1.** Experimental setup. BAG = bags; CVS = constant volume sampler; DIL = diluted; EFM = exhaust flow meter; FTIR = Fourier-transform infrared; IRLAM = infrared laser absorption modulation; SAO = smooth-approach orifice; TLP = tailpipe.

## 2.2. Instrumentation

Table 1 gives an overview of the instruments that were available in this measurement campaign. Their exact sampling position was given in Figure 1.

**Table 1.** Characteristics of instruments and principles of measurement.

Analyzer	BAG	DIL	TLP	FTIR #1	FTIR #2	IRLAM
Manufacturer	HORIBA	HORIBA	HORIBA	AVL	HORIBA	HORIBA
Model	MEXA-7400	MEXA-7400	MEXA-7100	Sesam i60	FTX-ONE	IRLAM PEMS
CO <sub>2</sub>	NDIR	NDIR	NDIR	FTIR	FTIR	QCL-IR
CO	NDIR	NDIR	NDIR	FTIR	FTIR	QCL-IR
NO <sub>x</sub> (NO + NO <sub>2</sub> )	CLD	CLD	CLD	FTIR	FTIR	QCL-IR
N <sub>2</sub> O	-	-	-	FTIR	FTIR	QCL-IR
NH <sub>3</sub>	-	-	-	FTIR	FTIR	QCL-IR
HCHO	-	-	-	FTIR	FTIR	QCL-IR
CH <sub>4</sub>	GC-FID	-	-	FTIR	FTIR	QCL-IR
Sampling line T (°C)	-	191	191	191	191	113
Analyser t <sub>10-90</sub> (s)	-	2.5	2.5	2.0	1.5 <sup>1</sup>	1.0 <sup>2</sup>
Q <sub>s</sub> (L/min)	-	11	11	6.5	3.5	3.3

<sup>1</sup> For NH<sub>3</sub> <3 s; <sup>2</sup> for NH<sub>3</sub> <1.5 s. CLD = chemiluminescence detection; DIL = diluted; FID = flame ionization detection; FTIR = Fourier-transform infrared; GC = gas chromatography; IRLAM = infrared laser absorption modulation; NDIR = non-dispersive infrared; QCL-IR = quantum cascade laser infrared; Q<sub>s</sub> = sample flow rate; TLP = tailpipe.

IRLAM, that stands for infrared laser absorption modulation, is the prototype PEMS based on quantum cascade laser infrared (QCL-IR) technology [23]. The analyzers unit weighed 33 kg, and the 6 m heated line another 6 kg, which made it suitable for on-road testing for both LD and HD applications. IRLAM measured CO, CO<sub>2</sub>, NO, NO<sub>2</sub>, N<sub>2</sub>O, NH<sub>3</sub>, CH<sub>4</sub>, and HCHO [21,22]. For CO and CH<sub>4</sub> the instrument measured on a low and a high range (Appendix A, Table A1), and then it allocated the value from one or the other analyzer based on the actual concentration. The instrument was factory calibrated. Span gases for all the measured species were used only to verify the span on a daily basis, but no adjustments were made, except when the test temperature changed from 23 °C to −7 °C. A bottle of N<sub>2</sub> was used for zero calibration of each analyzer prior to each test. IRLAM was located downstream of the PEMS exhaust flowmeter (EFM) and it was the first instrument sampling from the exhaust. The sampling rate of IRLAM was 3.3 L/min. A six-meter length heated line (113 °C) was used to connect the sampling point and the PEMS. The acquisition frequency was 10 Hz. The instrument was placed inside the climatic chamber, and thus it was operated at 23 °C or −7 °C depending on the test settings.

Downstream of the IRLAM, a FTX-ONE-CS (HORIBA, Kyoto, Japan) was placed [24]. This is a laboratory grade instrument that uses the Fourier-transform infrared (FTIR) spectrometer to measure the raw exhaust (abbreviated as FTIR #2) [20]. This instrument was factory calibrated and the same gas bottles used for IRLAM were used to check zero and span prior to the start of the campaign. The sampling rate was 3.5 L/min and the acquisition frequency was 5 Hz. FTIR #2 was connected to the sampling location with a heated line (191 °C) equipped with a heated pre-filter.

A second laboratory grade FTIR spectrometer was also used (Sesam i60 from AVL, Graz, Austria), abbreviated as FTIR #1. The sampling point of this instrument was immediately after the one of FTIR #2. A heated (191 °C) polytetrafluoroethylene sampling line was used to avoid water condensation. The sampling rate was 6.5 L/min and the acquisition rate was 1 Hz. The distances between three instruments (IRLAM, FTIR #1, FTIR #2) were short (around 5 cm between each other).

In VELA 2, the instruments measuring from the dilution tunnel (abbreviated as DIL) and from the bags (abbreviated as BAG) were MEXA-7400 benches from HORIBA that used non-dispersive infrared detection for CO and CO<sub>2</sub>, chemiluminescence detection for NO<sub>x</sub>, and flame ionization detection for total hydrocarbons (THC) and CH<sub>4</sub>. An additional gas bench from HORIBA (MEXA-7100) was used to measure the exhaust at the tailpipe

(abbreviated as TLP) [25]. CO and CO<sub>2</sub> were measured after removing the water content and a dry-to-wet correction was applied based on CO<sub>2</sub>, CO, and THC concentrations [26]. DIL and TLP measurements were performed at a rate of 10 Hz. HORIBA STARS VETS was used as automation and reporting software for the BAG, DIL, and TLP data, whereas all the other instruments (IRLAM, FTIR #1, FTIR #2) were used as standalone.

The exhaust flowrate was measured with the HORIBA PEMS using a dedicated exhaust flowmeter (EFM), based on a Pitot tube using the differential pressure measurement principle. The exhaust temperature was measured with a dedicated probe and it was used to correct the measured flowrate by the PEMS. The exhaust flowrate was also calculated using the differential air flow method (i.e., CVS—SAO) and the CO<sub>2</sub> tracer method, i.e., CVS flow divided by the dilution factor  $CO_{2,TLP}/(CO_{2,DIL}-CO_{2,air})$ . Details can be found elsewhere [27] and at the Appendix B. IRLAM and FTIR #2 were shipped to JRC before the beginning of the campaign, while the rest of the equipment were owned by JRC.

### 2.3. Vehicles and Fuels

Three vehicles were used in the test campaign (Table 2).

**Table 2.** Characteristics of vehicles.

Characteristics	D6	G6	G4
Vehicle category	M1	M1	M1
Cylinders/arrangement	4-inline	4-inline	4-inline
Combustion type	Compression ignition	Positive ignition	Positive ignition
Fuel type	Diesel	Gasoline	Gasoline
Injection type	Direct	Port-fuel	Port-fuel
Aspiration type	Turbocharged	Turbocharged	Natural aspiration
Engine displacement (cm <sup>3</sup> )	1998	1598	1108
ICE engine power (kW)	150	69	40
Electric engine V/power (kW)	48 V/13.3 kW	245 V/51 kW	-
Emission control technology	DOC, DPF, EGR, SCR, LNT	TWC, GPF	TWC
Transmission/gearbox	Automatic	Automatic	Manual
Test mass (kg)	1903	1635	1020
Registration date	July 2021	September 2022	August 2006
Mileage (km)	21,000	9000	25,700
Emission standard	Euro 6d-ISC-FCM	Euro 6d-ISC-FCM	Euro 4

DOC = Diesel oxidation catalyst; DPF = Diesel particulate filter; EGR = exhaust-gas recirculation; FCM = fuel consumption monitoring; GPF = gasoline particulate filter; ICE = internal combustion engine; ISC = in-service conformity; LNT = lean NO<sub>x</sub> trap; SCR = selective-catalytic reduction; TWC = three-way catalyst.

Two of them met the Euro 6d emissions standard and were selected as representative of Diesel (D6) and gasoline (G6) state-of-the-art technologies. D6 was a mild-hybrid combining a 2 L 150 kW internal combustion engine (ICE) and a 48 V battery system with a 13.3 kW e-motor. D6 was equipped with an exhaust-gas recirculation (EGR) system, a Diesel oxidation catalyst (DOC), a selective-catalytic reduction (SCR) system, a lean NO<sub>x</sub> trap (LNT), and a Diesel particulate filter (DPF). G6 was a mild-hybrid with a 1.6 L ICE with a 51 kW e-motor. As emission control systems it featured a three-way catalyst (TWC) and a gasoline particulate filter (GPF). The third vehicle was a Euro 4 gasoline vehicle equipped with a TWC only. Despite being sixteen years old it had relatively low mileage, featuring only 25,700 km on the odometer at the time of the campaign. Table 2 displays additional details of the tested vehicles.

A number of standard on-board diagnostics (OBD) channels were acquired through the vehicles' OBD ports, when available. G4 did not have an OBD port and thus no OBD data could be logged. The OBD communication with D6 had frequent glitches and most of the data were lost after 300–400 s of the tests.

All three vehicles used commercial fuels: Diesel B7 (D6) and gasoline E5 (G6 and G4). No other fuels were available for testing at the time the experimental campaign was performed.

#### 2.4. Protocol

The test campaign started with G6. This vehicle was tested over the worldwide harmonized light-vehicles test cycle (WLTC) with cold engine start, at ambient temperatures of 23 °C and −7 °C. In addition, a dynamic motorway test (BAB), characterized by sharp accelerations from 110 km/h to 130 km/h, and 80 km/h to 130 km/h, was driven in hot operating conditions (engine coolant temperature above 70 °C). The low speed, low load Transport for London (TfL) cycle was also driven at 23 °C and −7 °C. Finally, a 1.5 h long test simulating an aggressive driving but compliant with the real-driving emissions (RDE) driving dynamic regulation requirements was also driven on by G6 (RDE\_D). This test was driven to assess potential drift of analyzers over a relative longer drive than the other cycles.

D6 was driven on cold-started WLTC at 23 °C and −7 °C ambient temperature. The BAB and TfL cycles were driven at 23 °C. A DPF regeneration occurred at the end of one WLTC 23 °C and a constant speed 130 km/h test for 30 min was subsequently driven to allow for a complete regeneration. Finally, a 30-min, 28 km long, RDE on dyno cycle was driven combining urban, rural, and motorway drive (RDE\_S).

With G4, just two repetitions of cold-started WLTC 23 °C were performed. The main characteristics of the cycles can be found in Table 3, and more details elsewhere [28].

**Table 3.** Characteristics of the test cycles.

Cycle	WLTC	BAB	TfL	RDE_S	RDE_D
Distance (km)	23.2	24.9	8.8	28.3	91.7
Duration (s)	1800	800	2320	1830	5400
Mean speed (km/h)	46.2	111.5	13.7	54.9	61.0
Max speed (km/h)	131.3	131.1	51.8	130.7	143.6

BAB = Bundesautobahn (federal highway); D = dynamic; S = short; TfL = Transport for London; RDE = real-driving emissions; WLTC = worldwide harmonized light-vehicles test cycle.

#### 2.5. Calculations

After each test, the uncorrected data results from each instrument were checked for consistency. When obvious communication problems or implausible values were identified, the data of the instrument were voided. For example, for some tests, data were lost due to communication errors (three times FTIR #1, four times FTIR #2, two times BAG). All data were then down-sampled to 1 Hz frequency and synchronized using the CO concentration values as a reference. OBD data were synchronized with the dyno using the vehicle speed signal.

Mass emission rates in g/s were calculated for all the tailpipe instruments (IRLAM, FTIR #1, FTIR #2, TLP) using the exhaust flowrate as measured with EFM, as well as using the CO<sub>2</sub> tracer and the air flow difference methods. For consistency reasons the instruments were compared using the same exhaust flow rate (air flow differences); however, the differences between the exhaust flow methods will also be discussed. The dyno speed trace was used as source of driven distance to calculate the distance-specific emissions.

No corrections (e.g., for drift, or negatives) have been applied to the concentration measured of any of the instruments.

### 3. Results

Initially, real-time examples are given in order to better understand the integrated results. Then a summary of the differences among the instruments is given.

#### 3.1. Real Time Examples

Figure 2 plots examples of CO<sub>2</sub> concentrations. Figure 2a plots the CO<sub>2</sub> signals of the gasoline Euro 4 vehicle (G4) for a cold start WLTC. All instruments measured “wet” exhaust, except TLP which measured “dry” and then corrected with the dry-to-wet correction, as described in the light-duty Regulation (EU) 2017/1151. The IRLAM and FTIR #1 were

very close to each other (1% relative difference, e.g., 13.8% vs. 13.9% at time 120 s). The TLP was 8% lower, but after 400 s reached the same level as the other two instruments. The differences between “wet” and “dry” measuring instruments during cold start is well-known, and has to do with water condensation taking place at the surfaces of the vehicle’s tailpipe, which is not taken into account by the dry-to-wet equation, since the condensed amount is unknown. FTIR #2 was 7% higher (13.7% vs. 12.8%). This difference remained until the end of the test (not shown in the figure), thus it had to do with the instrument and not with the sampling position and possible differences in water condensation. The overestimation was also confirmed by comparing the integrated emissions with the bags and diluted concentrations (no figure shown; results will be summarized in the next section). Differences of the instruments compared to TLP of 4–6% during cold start were also found with the gasoline vehicles, which were 0% at the hot operation. FTIR #2 was 7% higher at both parts of the cycle (no figure shown).

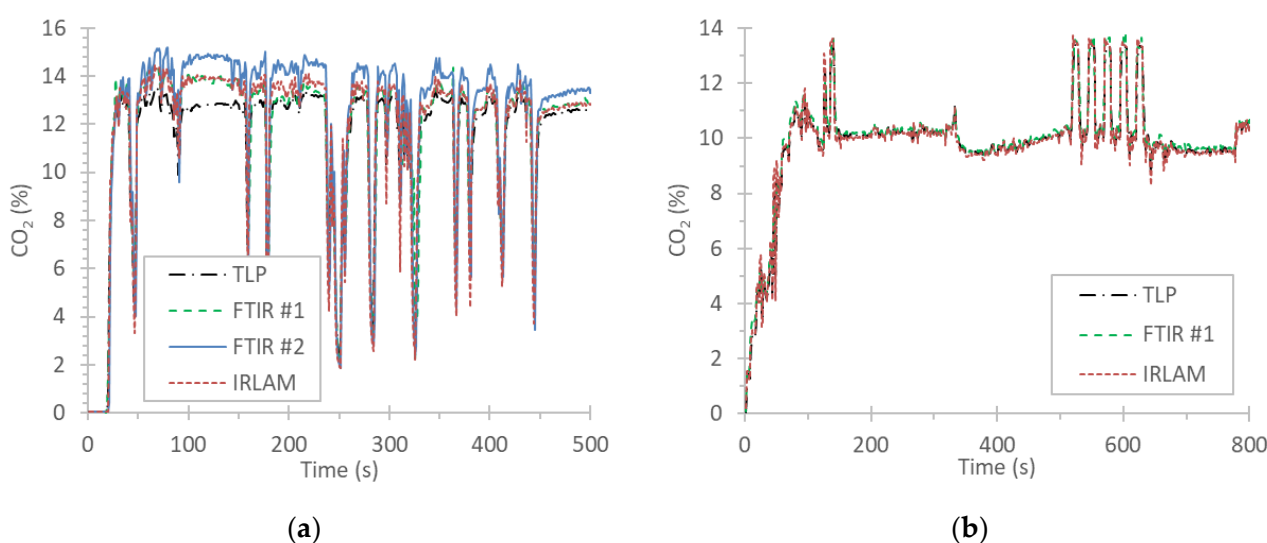
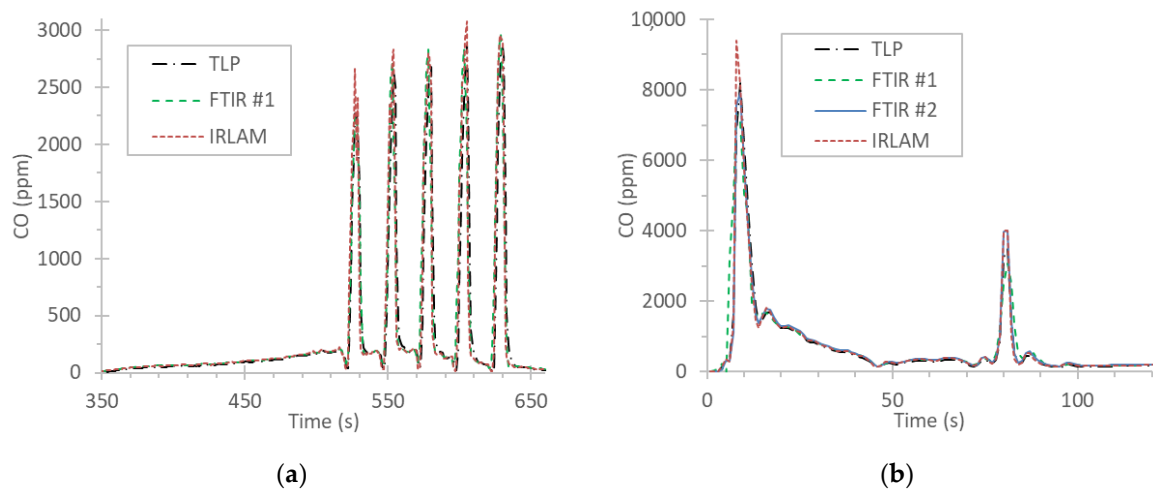


**Figure 2.** Real time CO<sub>2</sub> tailpipe concentrations during: (a) a cold start WLTC of the gasoline Euro 4 (G4) vehicle; (b) steady 130 km/h test with regeneration of the Diesel Euro 6 (D6) vehicle.

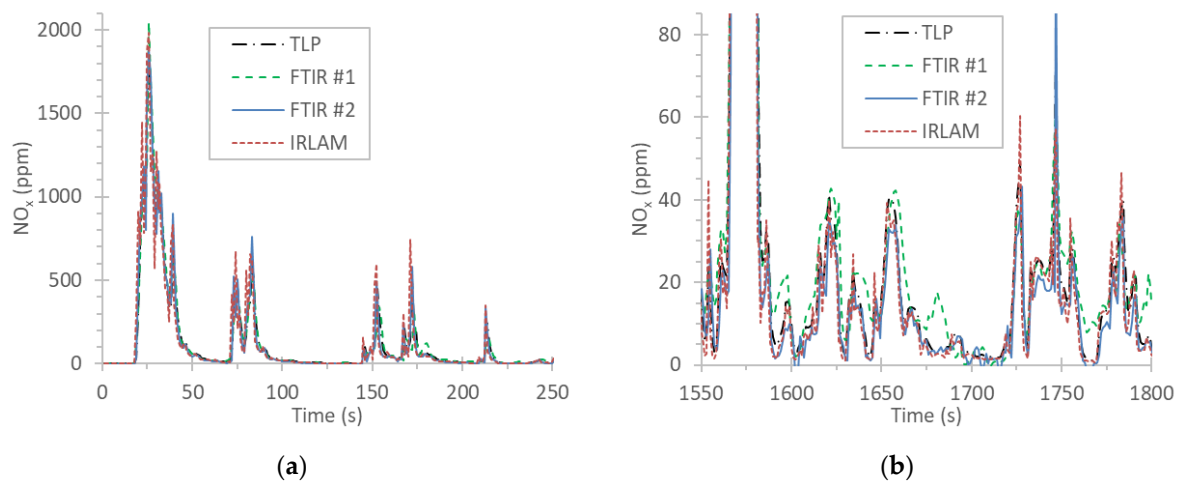
Figure 2b plots the CO<sub>2</sub> emissions of the Euro 6 Diesel vehicle (D6) during constant speed driving where a DPF regeneration took place. FTIR #2 was not available due to a technical problem. The agreement of the other instruments was very good (differences <1% from the mean).

Figure 3a plots CO concentrations of the D6 vehicle during the DPF regeneration at 130 km/h. The emissions ranged from 0 ppm up to 3000 ppm. The agreement of the instruments was very good. Figure 3b plots CO concentrations of the G6 during the first two minutes of a cold start WLTC. The agreement is very good with differences of 4–8% compared to the TLP in the first two minutes. Interestingly, this difference remained at the end of the test (within experimental uncertainty 2%), indicating that water contribution did not play a role as with CO<sub>2</sub>. Similarly, with the other gasoline vehicle the differences of the instruments to TLP during cold start and hot operation were similar.

Figure 4a plots the NO<sub>x</sub> (NO+NO<sub>2</sub>) concentrations at the tailpipe of the G4 vehicle for a cold start WLTC. The agreement of the four instruments was excellent over a wide range of concentrations (0–2000 ppm). Figure 4b plots the NO concentrations at low levels (note that the spikes have been cut due to the reduced y-axis scale), during the last 300 s of the same cycle. The agreement remained very good even at low levels.



**Figure 3.** Real time tailpipe concentrations: (a) CO over a steady 130 km/h test with regeneration with the Diesel Euro 6 (D6) vehicle; (b) Cold start WLTC with the gasoline Euro 6 (G6) vehicle.

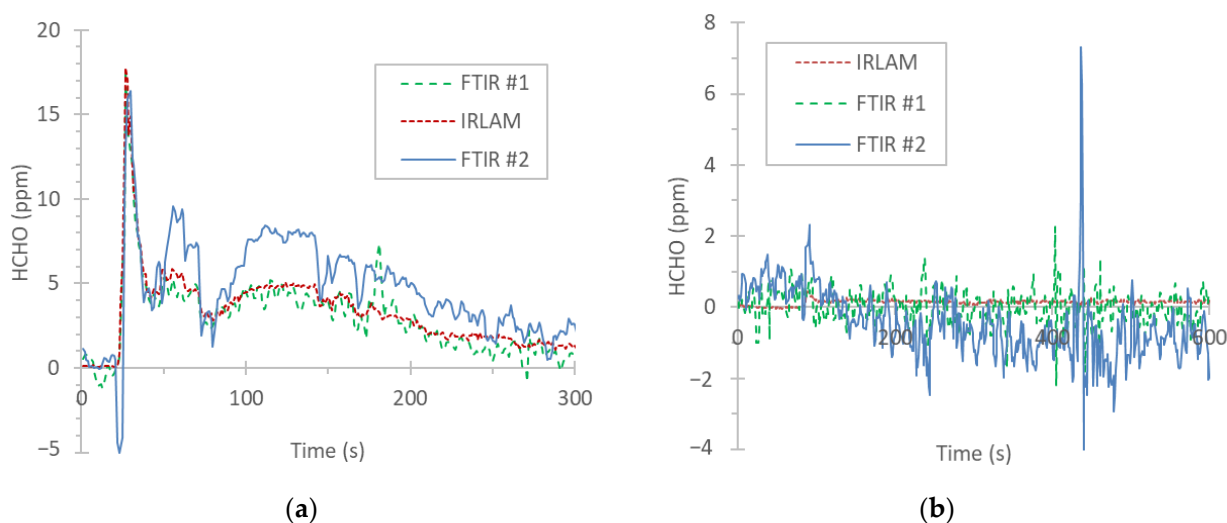


**Figure 4.** Real time tailpipe  $\text{NO}_x$  concentrations during a cold start WLTC of the gasoline Euro 4 (G4) vehicle: (a) cold start; (b) last 300 s.

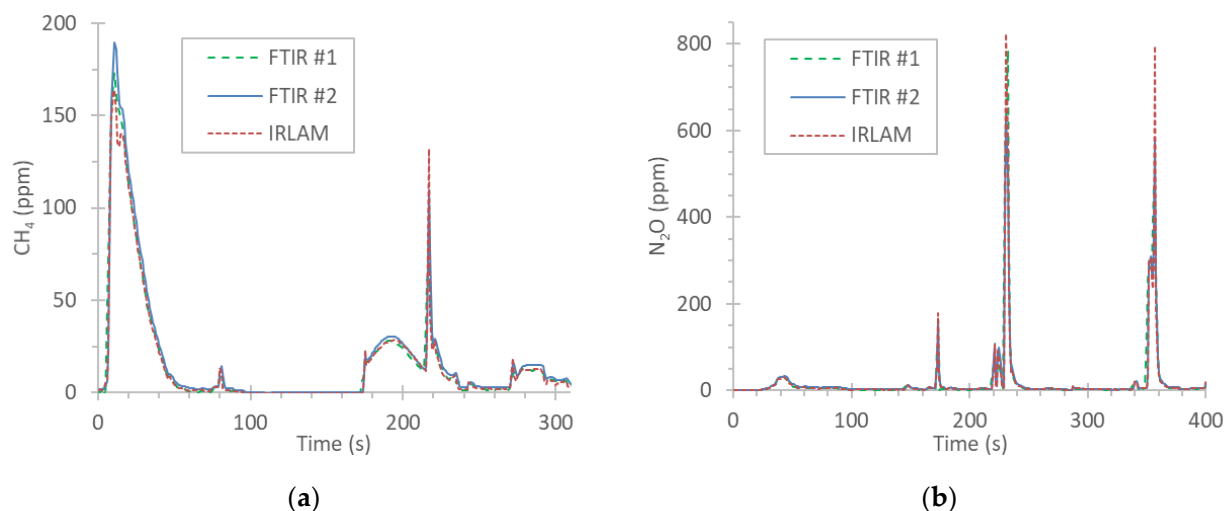
Figure 5a plots HCHO concentrations for the Euro 4 gasoline vehicle (G4) over the cold start of a WLTC. The agreement of the instruments during the first peak was very good. When the concentrations dropped to 5 ppm, FTIR #2 remained higher compared to the other two instruments, which were close to each other. After the first two minutes, the difference was around 2 ppm.

Figure 5b plots HCHO concentrations for the Euro 6 Diesel vehicle (D6). The IRLAM started with zero emissions ( $-0.01 \pm 0.02$ ), at approximately 85 s there was an increase, and then the emissions remained slightly elevated at  $0.14 (\pm 0.04)$  ppm, which could be true vehicle emissions. The two FTIRs were noisier. For example, FTIR #1 measured on average 0 ppm with one standard deviation of 0.45 ppm. FTIR #2 measured on average  $-0.5$  ppm with one standard deviation of 1 ppm.

Figure 6a plots  $\text{CH}_4$  concentrations of the gasoline Euro 6 (G6) vehicle over the cold start of a WLTC. There was a good agreement between the instruments, with FTIR #2 higher (12%) compared to the other two instruments, which were close to each other. At low concentrations IRLAM and FTIR #1 remained within 1 ppm, while FTIR #2 was 1–2 ppm higher.



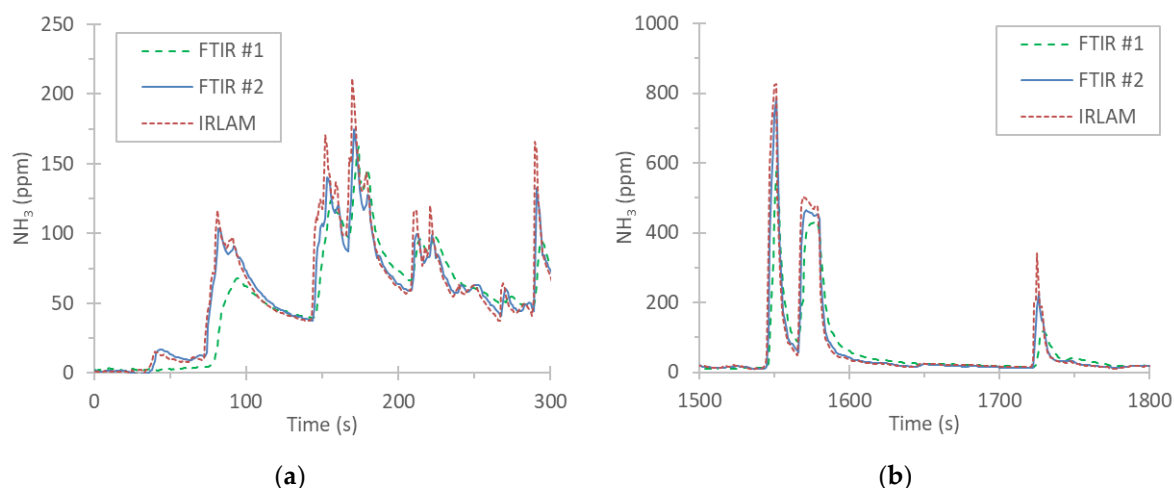
**Figure 5.** Real time tailpipe concentrations (a)  $\text{CH}_4$  over a cold start WLTC of the gasoline Euro 4 (G4) vehicle; (b) HCHO during a cold start RDE\_D of the Diesel Euro 6 (D6) vehicle.



**Figure 6.** Real time tailpipe concentrations (a)  $\text{CH}_4$  over a cold start WLTC of the gasoline Euro 6 (G6) vehicle; (b)  $\text{N}_2\text{O}$  over a cold start WLTC at  $-7\text{ }^\circ\text{C}$  of the Diesel Euro 6 (D6) vehicle.

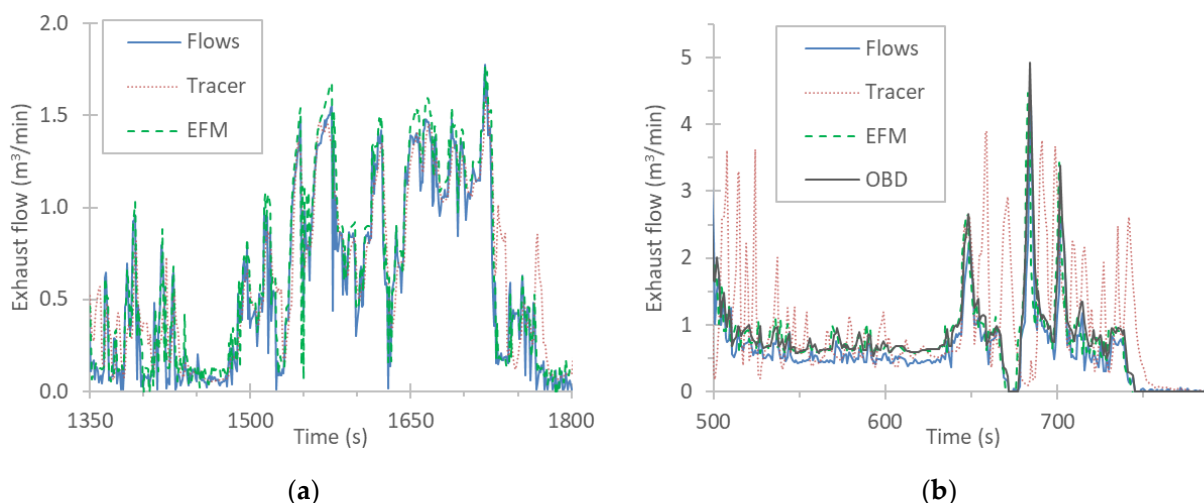
Figure 6b plots  $\text{N}_2\text{O}$  concentrations of the three instruments. The agreement was excellent (within  $\pm 6\%$  of their mean) over a wide range of concentrations (0–800 ppm).

Figure 7 plots the  $\text{NH}_3$  concentrations of the gasoline Euro 4 (G4) vehicle over the cold start (Figure 7a) and the last high speed part of the WLTC (Figure 7b). The average concentration of the complete cycle, estimated by IRLAM, was 40 ppm, corresponding to 17 mg/km. FTIR #2 and IRLAM correlated well to each other, with IRLAM measuring slightly higher (5%). FTIR #1 had in general lower and broader peaks. The slower response had to do with the higher  $t_{10-90}$  rise time of the analyzer (Table 1). Furthermore, during cold start some  $\text{NH}_3$  was “lost”: at the first 5 min FTIR #1 was 6% lower, while at the last 5 min of the test only 2% lower. It was not investigated where the losses could have taken place, but it is known that cold spots, for instance on the connection point, or the filter of FTIRs, can result in some  $\text{NH}_3$  losses.



**Figure 7.** Real time tailpipe NH<sub>3</sub> concentrations during a cold start WLTC of the gasoline Euro 4 (G4) vehicle: (a) cold start; (b) last 300 s.

Figure 8 plots the exhaust flow rate of the Euro 4 gasoline (G4) vehicle (Figure 8a) and the Euro 6 Diesel (D6) vehicle (Figure 8b). The measured flow with the exhaust flow meter (“EFM”) was close or higher than the flow calculated by flow differences (total tunnel flow CVS minus dilution air SAO) (“Flows”) or the CO<sub>2</sub> tracer method (“Tracer”). For these graphs the tailpipe extracted flow from the instruments was taken into account. The percentage of extracted flow was on average (for the WLTC) 7% for G4, 4% for G6, and 8% for D6. The highest variability was for D6: from 2% (highway) to 15% (urban). The EFM was close to the exhaust flow rate from the OBD that was available for D6. On average the differences were 4–9% (EFM higher). The tracer method had spikes during decelerations. This is known due to the fuel cut-offs and the differences in delays of the CO<sub>2</sub> lines (at tailpipe and dilution tunnel). The D6 had many such spikes in Figure 8b due to the dynamic behavior of the specific cycle.



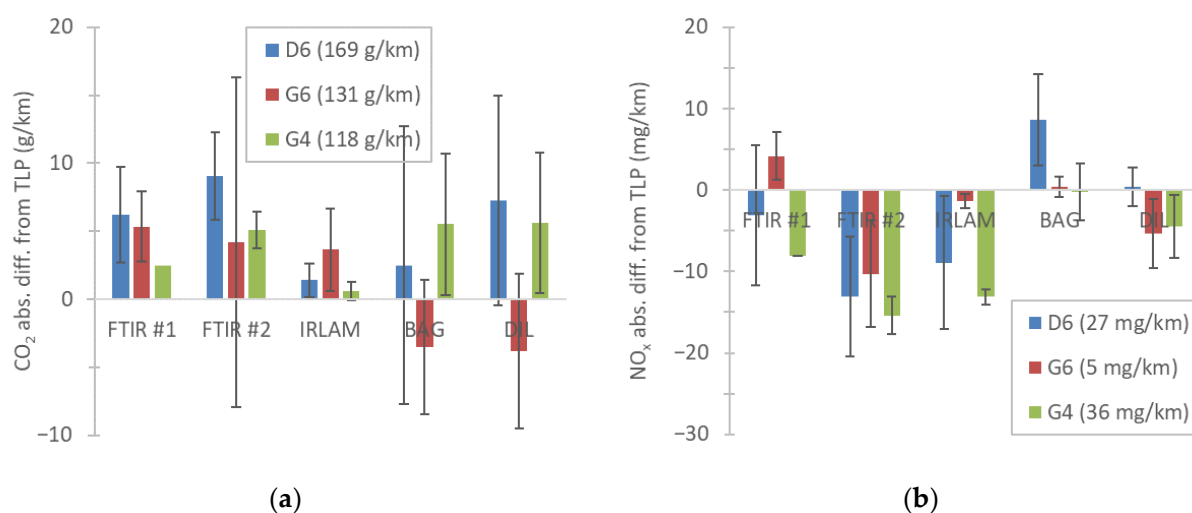
**Figure 8.** Exhaust flow rate measurements: (a) part of a WLTC with the Gasoline Euro 4 (G4) vehicle; (b) part of RDE\_D with the Diesel Euro 6 (D6) vehicle.

### 3.2. Integrated Results

This section summarizes the differences among the instruments (FTIR #1, FTIR #2, IRLAM, BAG, DIL, TLP) for the three vehicles (D6, G6, G4). The differences are given in absolute values (g/km or mg/km); however, the mean emission levels of each vehicle on the driven cycles are also given in the legend. The averages are from 8 tests (D6), 11 tests (G6), and 2 tests (G4). As reference, TLP was taken, and the same exhaust flow (flows

difference method) was used for all tailpipe instruments (FTIR #1, FTIR #2, IRLAM, TLP) to calculate the emissions. This way the impact of the exhaust flow on the results was minimized. TLP to BAG and DIL differences are also plotted in order to understand the difference of TLP from the current regulated method BAG. However, since BAG and DIL were not available for all pollutants, for consistency, it was decided to use TLP as reference. Furthermore, due to the high extracted flow from the tailpipe, the absolute levels (both at tailpipe and dilution tunnel) had some uncertainty that could impact the differences compared to BAG and DIL. For species that TLP was not measuring, the mean of the three tailpipe instruments (FTIR #1, FTIR #2, IRLAM) was considered as reference.

Figure 9a plots the CO<sub>2</sub> results. The mean differences ranged from −4 g/km to 9 g/km, while taking into account one standard deviation from −10 g/km to 15 g/km. Figure 9b plots the NO<sub>x</sub> results. The differences including one standard deviation were within ±15 mg/km. The higher difference of FTIR #2 (−20 mg/km in some cases) was due to the “offset” during the cycle due to interferences from other gases. It should be noted that the differences were of the same magnitude as the absolute levels for G6 (5 mg/km) or up to 40% of the emissions for the other two vehicles (emissions around 35 mg/km).



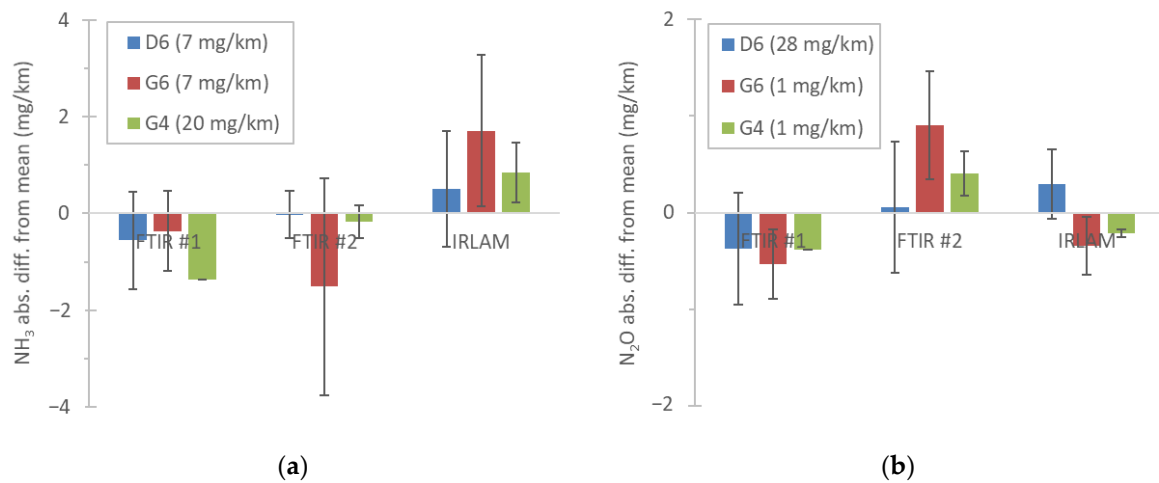
**Figure 9.** Absolute differences of the instruments from tailpipe analyzers (TLP): (a) CO<sub>2</sub>; (b) NO<sub>x</sub>. Each colored bar is a vehicle: Diesel Euro 6 (D6), gasoline Euro 6 (G6); gasoline Euro 4 (G4). Numbers in brackets are the average absolute emission levels over the driven cycles for each vehicle. Error bars give one standard deviation or max-min the G4.

Figure 10a summarizes the NH<sub>3</sub> results. The differences including one standard deviation were within ±3.5 mg/km, with typical mean differences within ±1.5 mg/km. Figure 10b summarizes the N<sub>2</sub>O results. The differences were in most cases within ±1 mg/km.

Figure 11a plots the results for CO. The tailpipe instruments had differences <75 mg/km from the TLP, while BAG and DIL up to 200 mg/km. For D6 and G6, which had relatively low CO emissions, the differences of the instruments were <50 mg/km. In general, the differences of the instruments were <15%. The higher difference from the tunnel analyzers indicates additional sources of uncertainty such as time alignment, exhaust flow uncertainty and dry-to-wet correction due to cold start condensation. Figure 11b plots the differences of the exhaust flow determination methods. In general, the differences were within 10%, with the exception of the Diesel vehicle that reached up to 20%.

To put the results into perspective, Table 4 gives an overview of the distance-specific emission differences and compares them with the emission levels of the examined vehicles and the European Commission proposal for LD vehicles in Euro 7. The Euro 7 limits include the measurement uncertainty of the instruments, thus the calibration and optimization of the vehicle emissions should consider the values of Table 4. Under Euro 7, a vehicle can be tested in the laboratory with laboratory grade equipment or on the road with portable

emissions measurement systems (PEMS), or combinations (e.g., in the laboratory with a random cycle using PEMS).



**Figure 10.** Absolute differences of the instruments from their mean: (a) NH<sub>3</sub>; (b) N<sub>2</sub>O. Each colored bar is a vehicle: Diesel Euro 6 (D6), gasoline Euro 6 (G6); gasoline Euro 4 (G4). Numbers in brackets are the average absolute emission levels. Error bars give one standard deviation or max-min in the case of the G4.

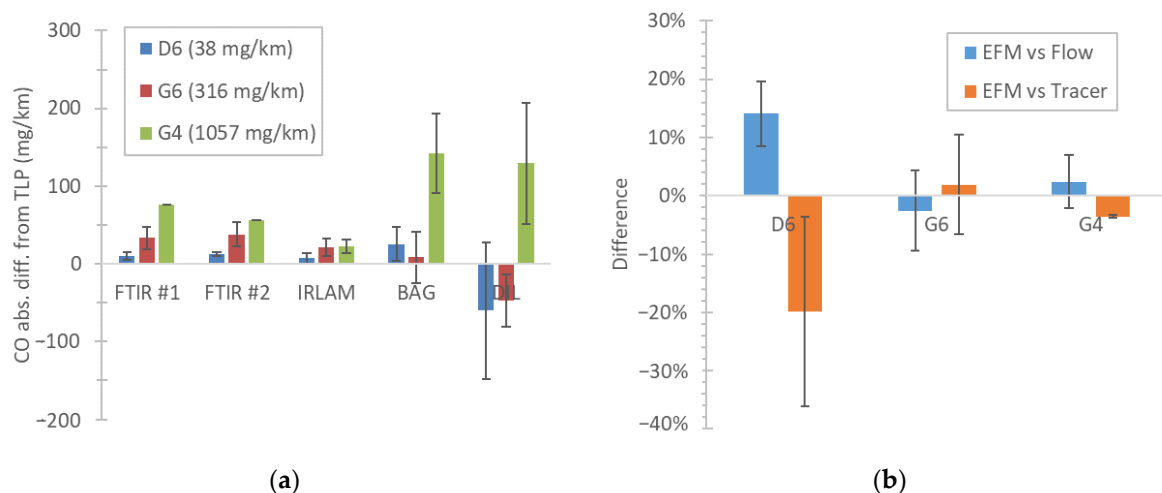


**Figure 11.** Absolute differences of the instruments from their mean: (a) CO; (b) exhaust flow.

**Table 4.** Measured absolute uncertainty with the reference (BAG, DIL) and new techniques (IRLAM, FTIR), in comparison with the proposed Euro 7 limits. The values were based on the comparisons with the TLP.

Component	Proposed Limit (Euro 7)	Examined Range (All Vehicles)	Uncertainty <sup>1</sup>
CO <sub>2</sub>	–	90–210 g/km	10–15 g/km
CO	500 mg/km	5–1085 mg/km	50 mg/km or 15% <sup>2</sup>
NO <sub>x</sub>	60 mg/km	1–72 mg/km	10–15 mg/km
CH <sub>4</sub> <sup>3</sup>	(32 mg/km)–	1–20 mg/km	1–2 mg/km
HCHO	–	0–1.7 mg/km	1 mg/km
NH <sub>3</sub>	20 mg/km	1–23 mg/km	1.5–3.5 mg/km
N <sub>2</sub> O	–	0–42 mg/km	1 mg/km
Exhaust flow <sup>4</sup>	–	0.1–2.3 m <sup>3</sup> /min	10–20%

<sup>1</sup> Mean difference plus one standard deviation; <sup>2</sup> Whichever is larger; <sup>3</sup> CH<sub>4</sub> has no limit, but the value is based on subtraction of THC and NMHC limits; <sup>4</sup> Mean over each cycle.

#### 4. Discussion

PEMS are not new; already in the '90s the first on-board measurement systems appeared [29,30]. For regulatory purposes, PEMS on-road testing was introduced in the United States of America (USA) in 2005 for heavy-duty vehicles in-use testing, avoiding the high costs of removing the engine from an in-use vehicle and testing it in the laboratory (see overview in [31]). In Europe, PEMS testing for heavy-duty vehicles was regulated in 2014. Shortly later, in 2017, PEMS testing was also added for light-duty vehicles in Europe, but the main reason was the differences between laboratory and on-road emissions [31,32].

Many studies have assessed the performance of PEMS. Some of the first studies used Monte Carlo simulations to randomly combine the various sources of PEMS measurement errors and determine the additive measurement allowance for the United States of America USA regulations [33]. In Europe a theoretical framework was set combining sources of uncertainty (e.g. analyzer, exhaust flow meter, drift) using the error propagation rule [8]. Experimental studies found differences with reference instruments on the order of 10–20 mg/km (or mg/kWh) for PEMS analyzers measuring NO<sub>x</sub> [34,35], or ±10% for FTIRs [20,36–43]; in line with our results. Regarding CO<sub>2</sub>, laboratory validations (i.e. comparison of PEMS with laboratory grade analyzers) in the literature reported differences well within 10% [44–47]. For FTIRs differences on the order of 5–10% (including one standard deviation) have been reported for CO<sub>2</sub> [38,40,42,43] and CO [40,42,43,47,48]. Our results were also on the order of 10–15% for the two gases. For NH<sub>3</sub> the reported differences of FTIRs were in general <5% [49,50], but with some cases reaching 20% [18,35,43]. Reported differences of FTIRs and QCLs (such as the IRLAM of our study) were also on the 5% range [51–53], sometimes reaching 20% [54]. We also noticed differences of the same magnitude. One of the FTIRs had lower levels and slower response. NH<sub>3</sub> can be easily “lost” when water condensation takes place (e.g., in the tubes until the sampling point), so the position of the instruments plays an important role [49]. However, in our case all instruments were very close to each other, so we believe its lower response had to do with the slower rise time of the analyzer and possibly some losses in the heated sampling line of the specific FTIR. For CH<sub>4</sub> the studies have indicated differences of ±5% [43,47,55]. Our results were on the 10% range. For formaldehyde the reported differences vary: from very small differences [40,56] up to 30% [57]. Few studies on N<sub>2</sub>O found differences of <10% [17,18,43]; in our case the differences were much smaller (1 mg/km up to 40 mg/km of N<sub>2</sub>O emissions).

The second-by-second plots revealed a few points that need attention. During cold start, condensation takes place in the aftertreatment devices and the tailpipe, thus the dry-to-wet equations of the regulation do not apply. This leads to differences between instruments measuring with and without drying of the exhaust gas. For these first minutes the CO<sub>2</sub> differences can be up to 10%, but the overall impact over a test cycle is typically <2% [26,44]. In our results the impact on CO<sub>2</sub> was up to 4% for the first 5 min (or 2 km), but for CO the impact was negligible. These difference for gases measured after drying (CO<sub>2</sub> and CO) should be considered when measuring very short cold-start trips, which are allowed under Euro 7.

Of particular interest was the low zero levels of IRLAM's HCHO. It was possible to measure vehicle emissions of 0.15 ppm, while the FTIRs were at their background levels: their standard deviation was 0.5 to 1 ppm vs. <0.05 ppm for the IRLAM. Zero levels of the instruments of our study are presented in Table A2. HCHO concentration levels above 2 ppm could be identified by all instruments. Another study from our laboratory noted this with heavy-duty vehicles: concentrations of <0.5 ppm could be detected only by the QCL, while at >1 ppm levels FTIRs and QCL were comparable [19]. The “noise” issue was of no importance for the rest pollutants because the cycles concentration levels were much higher.

Another important issue is the interference of various species (such as H<sub>2</sub>O and CO<sub>2</sub>) to the response of FTIRs. In our study we did not notice a particular issue. The differences of the NO<sub>x</sub> concentrations were at acceptable levels for the gasoline vehicle even at low levels.

We noticed however that “offsets” can appear when there is condensation and the sampling needs special attention. “Offsets” of a few ppm have also been reported in other studies for compressed natural gas (CNG) heavy duty engines [35] due to H<sub>2</sub>O interferences.

No specific differences in terms of measurement performance of IRLAM were observed between tests performed at 23 °C and −7 °C. It should also be also mentioned that no drift was seen for all instruments for any test (max duration 90 min), at least for the laboratory conditions (no vibrations, changes of pressure or temperature) of our study.

The exhaust flow measurements had differences on the order of 10%. None of the methods could be considered as reference and their uncertainties were at the same levels. The CO<sub>2</sub> tracer method had high spikes during fuel cut-offs resulting in unreliable values. Interestingly, the EFM was very close to the OBD exhaust flow signal and in between the tracer and flow difference methods.

In general, the “alternative” techniques (i.e., IRLAM and FTIR) demonstrated equivalent performance with the standard techniques of the laboratory grade analyzers. In particular, the IRLAM, even though a portable system, had small differences from the means of the rest instrument and in some cases an even better limit of detection.

## 5. Conclusions

In this study we compared NH<sub>3</sub>, N<sub>2</sub>O, CH<sub>4</sub>, and HCHO emissions between a prototype infrared laser absorption modulation (IRLAM) portable system, and two Fourier transform infrared (FTIR) spectrometers measuring at the tailpipe of one diesel and two gasoline fueled vehicles. Furthermore, CO<sub>2</sub>, CO, and NO<sub>x</sub> were also compared between IRLAM, FTIRs (i.e., “alternative” techniques) and laboratory grade analyzers measuring from the tailpipe, the dilution tunnel, and the bags (i.e., “standard” techniques). The tests covered a wide range of driving conditions and ambient temperatures of 23 °C and −7 °C.

The real time graphs did not reveal any particular issues, however attention should be paid to interferences for FTIRs when measuring NO<sub>x</sub>. One FTIR had slower response for NH<sub>3</sub> and the other FTIR overestimated the CO<sub>2</sub>. “Wet” and “dry” measurements had differences at cold start due to condensation of water taking place (4% for the first five minutes, but only for CO<sub>2</sub>). Low ambient temperature (−7 °C), dynamic driving, and DPF regeneration did not influence the performance of the instruments. The instruments did not drift during this measurement campaign at the laboratory conditions.

The differences were on the order of ±1 mg/km for HCHO, N<sub>2</sub>O, and CH<sub>4</sub>, and around ±2.5 mg/km for NH<sub>3</sub>. For NO<sub>x</sub> the differences were ±10–15 mg/km, for CO ±50 mg/km or ±15% (whichever was larger), and for CO<sub>2</sub> ±10–15 g/km. The exhaust flow meter (EFM) was within ±10% of the flows or tracer methods, and close to the OBD exhaust flow. The main conclusion is that the uncertainties, for both “standard” and “alternative” techniques are quite similar, and even for currently non regulated pollutants, are at still an acceptable level when considering the upcoming Euro 7 light-duty emission limits.

**Author Contributions:** Conceptualization, R.S.-B., V.V., B.G.; formal analysis, V.V., B.G.; writing—original draft preparation, B.G., V.V., R.S.-B.; writing—review and editing, Y.K., Y.O., T.K., A.M. All authors have read and agreed to the published version of the manuscript.

**Funding:** This research received no external funding.

**Data Availability Statement:** Data available upon request from the corresponding author.

**Acknowledgments:** The authors would like to acknowledge the VELA technical staff in particular Antonio Migneco, Marcos Otura, Philippe Le-Lijour, Maria Triikka, Sara Valentini, and Dominique Lesueur.

**Conflicts of Interest:** V.V., A.M., R.S.-B., B.G. declare no conflict of interest. The authors Y.K., Y.O. and T.K. are employed by companies selling PEMSs or FTIR systems, but they were not involved in the collection or evaluation of the data.

## Abbreviations

BAB	Bundesautobahn (federal highway);
BAG	bags
C	concentration
CH <sub>4</sub>	methane
CLD	chemiluminescence detection
CNG	compressed natural gas
CO	carbon monoxide
CO <sub>2</sub>	carbon dioxide
CVS	constant volume sampling
DA	dilution air
DIL	diluted
DOC	Diesel oxidation catalyst
DPF	Diesel particulate filter
EFM	exhaust flow meter
EGR	exhaust-gas recirculation
EU	European Union
FCM	fuel consumption monitoring
FID	flame ionization detection
FTIR	Fourier-transform infrared
GC	gas chromatography
GPF	gasoline particulate filter
GWP	global warming potential
HCHO	formaldehyde
HD	heavy-duty
IARC	International Agency for Research on Cancer
ICE	internal combustion engine
IPCC	Intergovernmental Panel on Climate Change
IRLAM	infrared laser absorption modulation
ISC	in-service conformity
JRC	Joint Research Center
LD	light-duty
LNT	lean NO <sub>x</sub> trap
m	mass rate
N <sub>2</sub> O	nitrous oxide
NDIR	non-dispersive infrared
NH <sub>3</sub>	ammonia
NMHC	non-methane hydrocarbons
NMOG	non-methane organic gases
NO <sub>2</sub>	nitrogen dioxide
NO <sub>x</sub>	nitrogen oxides
OBD	on-board diagnostics
PEMS	portable emissions measurement system
PM	particulate matter
Q	flow rate
QCL-IR	quantum cascade laser infrared
RDE	real-driving emissions
RDE_D	real-driving emissions dynamic
RDE_S	real-driving emissions short
SAO	smooth-approach orifice
SCR	selective-catalytic reduction
TfL	Transport for London
THC	total hydrocarbons
TLP	tailpipe
TWC	three-way catalyst
VELA	vehicle emissions laboratory
WHO	World Health Organization
WLTC	worldwide harmonized light-vehicles test cycle

## Appendix A

Measurement ranges (Table A1) and zero levels (Table A2) of instruments used in this study. For some instruments and species more ranges are available (distinguished by “/”). In this case the zero level was determined with the lowest range. The zero level was defined as two standard deviations of “zero” gas (N<sub>2</sub>) measurement from the sampling line over 30 s with the frequency of the actual tests. For FTIR #2, typical values are reported because the instrument was not available during the zero tests.

**Table A1.** Indicative measurement ranges.

Analyzer	BAG	DIL	TLP	FTIR #1	FTIR #2	IRLAM
Manufacturer	HORIBA	HORIBA	HORIBA	AVL	HORIBA	HORIBA
Model	MEXA-7400	MEXA-7400	MEXA-7100	Sesam i60	FTX-ONE	IRLAM PEMS
CO <sub>2</sub>	1%/5%	3%	20%	1%/20%	1%/5%/20%	20%
CO	10/200/500	1000	12%	50/8000/10%	200/5000/10%	1%/12%
NO	-	-	-	50/1000/1%	200/1000/5000	2000
NO <sub>2</sub>	-	-	-	25/1000	200	800
NO <sub>x</sub>	20/50	500	500/1%	-	-	-
N <sub>2</sub> O	-	-	-	25/1000	200	1000
NH <sub>3</sub>	-	-	-	50/1000	100/1000	1500
HCHO	-	-	-	20/1000	500	500
CH <sub>4</sub>	5/10	-	-	50/1000	500/1%	2000/1%

DIL = diluted; FTIR = Fourier-transform infrared; IRLAM = infrared laser absorption modulation; TLP = tailpipe.

## Appendix B

In laboratories, the exhaust flow of a vehicle ( $Q_{TLP}$ ) is mixed with dilution air ( $Q_{DA}$ ) in a dilution tunnel. The total flow rate is constant and determined by a constant volume sampler (CVS) ( $Q_{DIL}$ ). Note that here DIL would correspond to CVS and dilution air (DA) corresponds to SAO from in Figure 1. The concentration of a pollutant at the tailpipe ( $C_{TLP}$ ) will decrease in the dilution tunnel ( $C_{DIL}$ ) depending on the dilution and the background contribution from the dilution air. Figure A1 presents two cases: in one case there was no extraction from the tailpipe, while in the second some flow was extracted.

For the case without any extraction (Figure A1a), neglecting the contribution from the dilution air (i.e.,  $C_{DA} = 0$ ) and the unit conversions, the mass rate of the pollutant ( $m_{TLP}$ ) can be calculated:

**Table A2.** Zero levels defined as two standard deviations of 30 s measurement of zero gas (N<sub>2</sub>) at the inlet of the sampling lines (except IRLAM at the inlet of the calibration line). The values were obtained at the lowest range. Not products specifications.

Analyzer	BAG	DIL <sup>1</sup>	TLP <sup>1</sup>	FTIR #1 <sup>2</sup>	FTIR #2 <sup>3</sup>	IRLAM <sup>4</sup>
Manufacturer	HORIBA	HORIBA	HORIBA	AVL	HORIBA	HORIBA
Model	MEXA-7400	MEXA-7400	MEXA-7100	Sesam i60	FTX-ONE	IRLAM PEMS
CO <sub>2</sub>	n.a.	2.40	2.60	130	0.64	39.00
CO	n.a.	0.04	2.70	1.2	0.09	0.84
NO	-	-	-	1.0	0.35	0.19
NO <sub>2</sub>	-	-	-	0.4	0.05	0.09
NO <sub>x</sub>	n.a.	0.03	0.03	-	-	-
N <sub>2</sub> O	-	-	-	0.4	0.06	0.07
NH <sub>3</sub>	-	-	-	0.5	0.05	0.07
HCHO	-	-	-	0.6	0.20	0.04
CH <sub>4</sub>	n.a.	-	-	0.5	0.06	0.16

<sup>1</sup> Measurement with 10 Hz sampling frequency with the unit used in this study. <sup>2</sup> Measurement with 1 Hz sampling frequency with the unit used in this study. <sup>3</sup> Typical values with 5 Hz sampling frequency. <sup>4</sup> Measurement with 10 Hz sampling frequency with the unit used in this study. DIL = diluted; FTIR = Fourier-transform infrared; IRLAM = infrared laser absorption modulation; n.a. = not available; TLP = tailpipe.

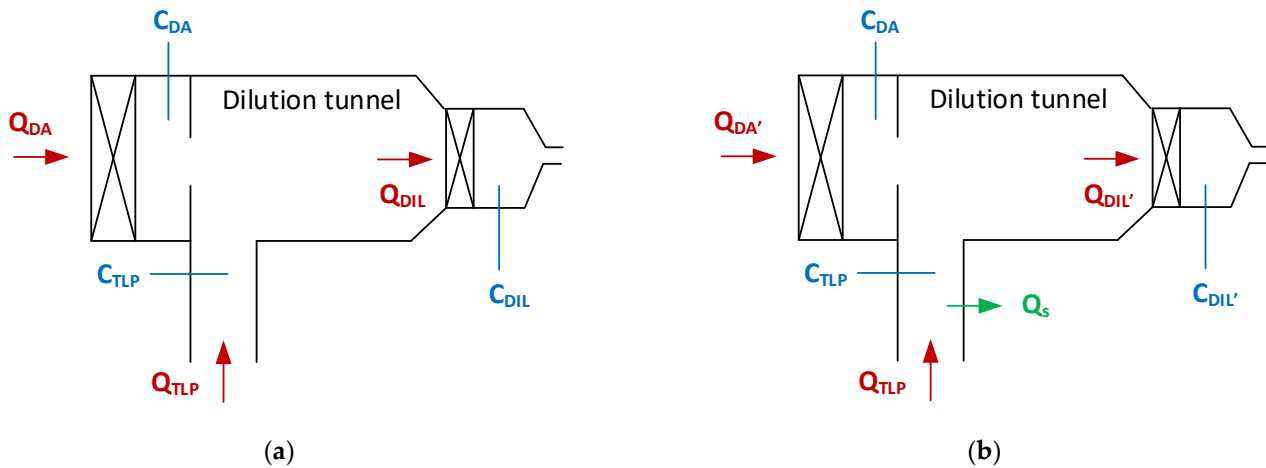


**Figure A1.** Impact of extracted flow  $Q_s$  on concentrations and flows: (a) no extracted flow; (b) with extracted flow from the tailpipe.

$$m_{TLP} = C_{TLP} \times Q_{TLP} \quad (A1)$$

The concentration of the pollutant at the tailpipe  $C_{TLP}$  is measured by an analyzer. The exhaust flow of the vehicle  $Q_{TLP}$  can be found as:

$$Q_{TLP} = Q_{DIL} - Q_{DA} \quad (A2)$$

The same result can be found by using the dilution tunnel measurements:

$$m_{DIL} = C_{DIL} \times Q_{DIL} \quad (A3)$$

The dilution tunnel flow  $Q_{DIL}$  is known and the  $C_{DIL}$  is measured by an analyzer. The two masses should be equal ( $m_{TLP} = m_{DIL}$ ). Furthermore, the dilution factor (DF) is:

$$DF = Q_{DIL}/Q_{TLP} = C_{TLP}/C_{DIL} \quad (A4)$$

For the case with a flow extraction ( $Q_s$ ) (Figure A1b):

$$Q_{TLP} = Q_{DIL} - Q_{DA'} + Q_s \quad (A5)$$

However, if the extracted flow  $Q_s$  is not considered, then the calculated exhaust flow ( $Q_{TLP,unc}$ ) will be lower:

$$Q_{TLP,unc} = Q_{DIL} - Q_{DA'} = Q_{TLP} - Q_s \quad (A6)$$

Consequently, the calculated mass of the pollutant will be underestimated if the uncorrected exhaust flow is used:

$$m_{TLP,unc} = C_{TLP} \times Q_{TLP,unc} \quad (A7)$$

Similarly, the mass calculated from the dilution tunnel data will also be underestimated if the extracted mass is not considered:

$$m_{DIL,unc} = C_{DIL'} \times Q_{DIL} \quad (A8)$$

$$m_s = C_{TLP} \times Q_s \quad (A9)$$

$$m_{DIL} = m_{DIL,unc} + m_s \quad (A10)$$

Interestingly, not correcting for the extracted mass results in equivalent results when using tailpipe or dilution tunnel data: From Equation (A7), using Equation (A6):

$$m_{\text{TLP,unc}} = C_{\text{TLP}} \times (Q_{\text{TLP}} - Q_s) = C_{\text{TLP}} \times Q_{\text{TLP}} - C_{\text{TLP}} \times Q_s = m_{\text{TLP}} - m_s \quad (\text{A11})$$

The key conclusion is that the extracted flow has to be taken into account when the absolute levels are of importance. When comparing tailpipe with dilution tunnel emissions, in order to have comparable results, it is important to either take into account the extracted flow in both positions or ignore it in both positions. Additional extractions from the dilution tunnel or combination of methods to calculate the emissions (both flow and tracer) will result in deviations.

## References

1. European Environmental Agency (EEA). *Air Quality in Europe 2022. Report No. 05/2022*; ISBN 978-92-9480-515-7. Available online: <https://www.eea.europa.eu/publications/air-quality-in-europe-2022> (accessed on 30 January 2023).
2. Eurostat Mortality and Life Expectancy Statistics. Available online: [https://ec.europa.eu/eurostat/statistics-explained/index.php?title=mortality\\_and\\_life\\_expectancy\\_statistics2022](https://ec.europa.eu/eurostat/statistics-explained/index.php?title=mortality_and_life_expectancy_statistics2022) (accessed on 30 January 2023).
3. DieselNet Emission Standards. Available online: <https://dieselnet.com/standards/> (accessed on 30 January 2023).
4. Giechaskiel, B.; Melas, A.; Martini, G.; Dilara, P. Overview of Vehicle Exhaust Particle Number Regulations. *Processes* **2021**, *9*, 2216. [[CrossRef](#)]
5. European Environmental Agency (EEA). Air Pollutant Emissions Data Viewer (Gothenburg Protocol, LRTAP Convention) 1990–2020. Available online: <https://www.eea.europa.eu/data-and-maps/dashboards/air-pollutant-emissions-data-viewer-42021> (accessed on 30 January 2023).
6. European Commission. Joint Research Centre. *On-Road Testing with Portable Emissions Measurement Systems (PEMS): Guidance Note for Light Duty Vehicles*; Publications Office: Luxembourg, 2018.
7. European Commission. Joint Research Centre. Institute for Energy and Transport. *PEMS Based In-Service Testing: Practical Recommendations for Heavy Duty Engines/Vehicles*; Publications Office: Luxembourg, 2015.
8. Giechaskiel, B.; Clairotte, M.; Valverde-Morales, V.; Bonnel, P.; Kregar, Z.; Franco, V.; Dilara, P. Framework for the Assessment of PEMS (Portable Emissions Measurement Systems) Uncertainty. *Environ. Res.* **2018**, *166*, 251–260. [[CrossRef](#)]
9. Leso, V.; Macrini, M.C.; Russo, F.; Iavicoli, I. Formaldehyde Exposure and Epigenetic Effects: A Systematic Review. *Appl. Sci.* **2020**, *10*, 2319. [[CrossRef](#)]
10. Wang, M.; Hu, K.; Chen, W.; Shen, X.; Li, W.; Lu, X. Ambient Non-Methane Hydrocarbons (NMHCs) Measurements in Baoding, China: Sources and Roles in Ozone Formation. *Atmosphere* **2020**, *11*, 1205. [[CrossRef](#)]
11. Zhu, L.; Henze, D.K.; Bash, J.O.; Cady-Pereira, K.E.; Shephard, M.W.; Luo, M.; Capps, S.L. Sources and Impacts of Atmospheric NH<sub>3</sub>: Current Understanding and Frontiers for Modeling, Measurements, and Remote Sensing in North America. *Curr. Pollut. Rep.* **2015**, *1*, 95–116. [[CrossRef](#)]
12. European Commission Euro 7 Proposal. Available online: [https://single-market-economy.ec.europa.eu/sectors/automotive-industry/environmental-protection/emissions-automotive-sector\\_en2022](https://single-market-economy.ec.europa.eu/sectors/automotive-industry/environmental-protection/emissions-automotive-sector_en2022) (accessed on 30 January 2023).
13. Selleri, T.; Melas, A.D.; Joshi, A.; Manara, D.; Perujo, A.; Suarez-Bertoa, R. An Overview of Lean Exhaust DeNO<sub>x</sub> Aftertreatment Technologies and NO<sub>x</sub> Emission Regulations in the European Union. *Catalysts* **2021**, *11*, 404. [[CrossRef](#)]
14. Martinovic, F.; Castoldi, L.; Deorsola, F.A. Aftertreatment Technologies for Diesel Engines: An Overview of the Combined Systems. *Catalysts* **2021**, *11*, 653. [[CrossRef](#)]
15. Castoldi, L. An Overview on the Catalytic Materials Proposed for the Simultaneous Removal of NO<sub>x</sub> and Soot. *Materials* **2020**, *13*, 3551. [[CrossRef](#)]
16. Rood, S.; Eslava, S.; Manigrasso, A.; Bannister, C. Recent Advances in Gasoline Three-Way Catalyst Formulation: A Review. Proceedings of the Institution of Mechanical Engineers, Part D. *J. Automob. Eng.* **2020**, *234*, 936–949. [[CrossRef](#)]
17. Selleri, T.; Gioria, R.; Melas, A.D.; Giechaskiel, B.; Forloni, F.; Mendoza Villafuerte, P.; Demuynck, J.; Bosteels, D.; Wilkes, T.; Simons, O.; et al. Measuring Emissions from a Demonstrator Heavy-Duty Diesel Vehicle under Real-World Conditions—Moving Forward to Euro VII. *Catalysts* **2022**, *12*, 184. [[CrossRef](#)]
18. Suarez-Bertoa, R.; Gioria, R.; Selleri, T.; Lilova, V.; Melas, A.; Onishi, Y.; Franzetti, J.; Forloni, F.; Perujo, A. NH<sub>3</sub> and N<sub>2</sub>O Real World Emissions Measurement from a CNG Heavy Duty Vehicle Using On-Board Measurement Systems. *Appl. Sci.* **2021**, *11*, 10055. [[CrossRef](#)]
19. Suarez-Bertoa, R.; Selleri, T.; Gioria, R.; Melas, A.D.; Ferrarese, C.; Franzetti, J.; Arlitt, B.; Nagura, N.; Hanada, T.; Giechaskiel, B. Real-Time Measurements of Formaldehyde Emissions from Modern Vehicles. *Energies* **2022**, *15*, 7680. [[CrossRef](#)]
20. Giechaskiel, B.; Clairotte, M. Fourier Transform Infrared (FTIR) Spectroscopy for Measurements of Vehicle Exhaust Emissions: A Review. *Appl. Sci.* **2021**, *11*, 7416. [[CrossRef](#)]

21. Onishi, Y.; Hamauchi, S.; Shibuya, K.; McWilliams-Ward, K.; Akita, M.; Tsurumi, K. *Development of On-Board NH<sub>3</sub> and N<sub>2</sub>O Analyzer Utilizing Mid-Infrared Laser Absorption Spectroscopy*; SAE Technical Paper 2021-01-0610; SAE: Warrendale, PA, USA, 2021. [[CrossRef](#)]
22. Hara, K.; Shibuya, K.; Nagura, N.; Hanada, T.; Tsurumi, K. *Formaldehydes Measurement Using Laser Spectroscopic Gas Analyzer*; SAE Technical Paper 2021-01-0604; SAE: Warrendale, PA, USA, 2021. [[CrossRef](#)]
23. Shibuya, K.; Podzorov, A.; Matsuhama, M.; Nishimura, K.; Magari, M. High-Sensitivity and Low-Interference Gas Analyzer with Feature Extraction from Mid-Infrared Laser Absorption-Modulated Signal. *Meas. Sci. Technol.* **2021**, *32*, 035201. [[CrossRef](#)]
24. Lamas, J.E.; Hara, K.; Mori, Y. *Optimization of Automotive Exhaust Sampling Parameters for Evaluation of After-Treatment Systems Using FTIR Exhaust Gas Analyzers*; SAE Technical Paper 2019-01-0746; SAE: Warrendale, PA, USA, 2019. [[CrossRef](#)]
25. Sherman, M.T.; Chase, R.; Mauti, A.; Rauker, Z.; Silvis, W. Evaluation of Horiba MEXA 7000 Bag Bench Analyzers for Single Range Operation. *SAE Trans.* **1999**, *108*, 90–111.
26. Giechaskiel, B.; Zardini, A.A.; Clairotte, M. Exhaust Gas Condensation during Engine Cold Start and Application of the Dry-Wet Correction Factor. *Appl. Sci.* **2019**, *9*, 2263. [[CrossRef](#)]
27. Giechaskiel, B.; Zardini, A.A.; Lahde, T.; Clairotte, M.; Forloni, F.; Drossinos, Y. Identification and Quantification of Uncertainty Components in Gaseous and Particle Emission Measurements of a Moped. *Energies* **2019**, *12*, 4343. [[CrossRef](#)]
28. Giechaskiel, B.; Valverde, V.; Kontses, A.; Melas, A.; Martini, G.; Balazs, A.; Andersson, J.; Samaras, Z.; Dilara, P. Particle Number Emissions of a Euro 6d-Temp Gasoline Vehicle under Extreme Temperatures and Driving Conditions. *Catalysts* **2021**, *11*, 607. [[CrossRef](#)]
29. Kelly, N.A.; Groblicki, P.J. Real-World Emissions from a Modern Production Vehicle Driven in Los Angeles. *Air Waste* **1993**, *43*, 1351–1357. [[CrossRef](#)]
30. Jetter, J.; Maeshiro, S.; Hacho, S.; Klebba, R. Development of an On-Board Analyzer for Use on Advanced Low Emission Vehicles. *SAE Trans.* **2000**, *109*, 755–762.
31. Giechaskiel, B.; Bonnel, P.; Perujo, A.; Dilara, P. Solid Particle Number (SPN) Portable Emissions Measurement Systems (PEMS) in the European Legislation: A Review. *Int. J. Environ. Res. Public Health* **2019**, *16*, 4819. [[CrossRef](#)] [[PubMed](#)]
32. Weiss, M.; Bonnel, P.; Kühlwein, J.; Provenza, A.; Lambrecht, U.; Alessandrini, S.; Carriero, M.; Colombo, R.; Forni, F.; Lanappe, G.; et al. Will Euro 6 Reduce the NO<sub>x</sub> Emissions of New Diesel Cars?—Insights from on-Road Tests with Portable Emissions Measurement Systems (PEMS). *Atmos. Environ.* **2012**, *62*, 657–665. [[CrossRef](#)]
33. Buckingham, J.P.; Mason, R.L.; Spears, M.W. Determination of PEMS Measurement Allowances for Gaseous Emissions Regulated Under the Heavy-Duty Diesel Engine In-Use Testing Program Part 2—Statistical Modeling and Simulation Approach. *SAE Int. J. Fuels Lubr.* **2009**, *2*, 422–434. [[CrossRef](#)]
34. Cao, T.; Durbin, T.D.; Cocker, D.R.; Wanker, R.; Schimpl, T.; Pointner, V.; Oberguggenberger, K.; Johnson, K.C. A Comprehensive Evaluation of a Gaseous Portable Emissions Measurement System with a Mobile Reference Laboratory. *Emiss. Control. Sci. Technol.* **2016**, *2*, 173–180. [[CrossRef](#)]
35. Giechaskiel, B.; Jakobsson, T.; Karlsson, H.L.; Khan, M.Y.; Kronlund, L.; Otsuki, Y.; Bredenbeck, J.; Handler-Matejka, S. Assessment of On-Board and Laboratory Gas Measurement Systems for Future Heavy-Duty Emissions Regulations. *Int. J. Environ. Res. Public Health* **2022**, *19*, 6199. [[CrossRef](#)] [[PubMed](#)]
36. Daham, B.; Andrews, G.E.; Li, H.; Ballesteros, R.; Bell, M.C.; Tate, J.; Ropkins, K. *Application of a Portable FTIR for Measuring On-Road Emissions*; SAE Technical Paper 2005-01-0676; SAE: Warrendale, PA, USA, 2005. [[CrossRef](#)]
37. Li, H.; Ropkins, K.; Andrews, G.E.; Daham, B.; Bell, M.; Tate, J.; Hawley, G. *Evaluation of a FTIR Emission Measurement System for Legislated Emissions Using a SI Car*; SAE Technical Paper; SAE: Warrendale, PA, USA, 2006; ISBN 0-7680-1803-X.
38. Wallner, T.; Frazee, R. *Study of Regulated and Non-Regulated Emissions from Combustion of Gasoline, Alcohol Fuels and Their Blends in a DI-SI Engine*; SAE Technical Paper 2010-01-1571; SAE: Warrendale, PA, USA, 2010. [[CrossRef](#)]
39. Czerwinski, J.; Comte, P.; Güdel, M.; Mayer, A.; Lemaire, J.; Reutimann, F.; Berger, A.H. *Investigations of NO<sub>2</sub> in Legal Test Procedure for Diesel Passenger Cars*; SAE Technical Paper 2015-24-2510; SAE: Warrendale, PA, USA, 2015. [[CrossRef](#)]
40. Zhang, F.; Wang, J.; Tian, D.; Wang, J.-X.; Shuai, S.-J. Research on Unregulated Emissions from an Alcohols-Gasoline Blend Vehicle Using FTIR, HPLC and GC-MS Measuring Methods. *SAE Int. J. Engines* **2013**, *6*, 1126–1137. [[CrossRef](#)]
41. Olsen, D.B.; Kohls, M.; Arney, G. Impact of Oxidation Catalysts on Exhaust NO<sub>2</sub>/NO<sub>x</sub> Ratio from Lean-Burn Natural Gas Engines. *J. Air Waste Manag. Assoc.* **2010**, *60*, 867–874. [[CrossRef](#)]
42. Vojtišek-Lom, M.; Beránek, V.; Klír, V.; Jindra, P.; Pechout, M.; Voříšek, T. On-Road and Laboratory Emissions of NO, NO<sub>2</sub>, NH<sub>3</sub>, N<sub>2</sub>O and CH<sub>4</sub> from Late-Model EU Light Utility Vehicles: Comparison of Diesel and CNG. *Sci. Total Environ.* **2018**, *616–617*, 774–784. [[CrossRef](#)]
43. Suarez-Bertoa, R.; Pechout, M.; Vojtišek, M.; Astorga, C. Regulated and Non-Regulated Emissions from Euro 6 Diesel, Gasoline and CNG Vehicles under Real-World Driving Conditions. *Atmosphere* **2020**, *11*, 204. [[CrossRef](#)]
44. Varela, R.; Giechaskiel, B.; Sousa, L.; Duarte, G. Comparison of Portable Emissions Measurement Systems (PEMS) with Laboratory Grade Equipment. *Appl. Sci.* **2018**, *8*, 1633. [[CrossRef](#)]
45. Giechaskiel, B.; Casadei, S.; Mazzini, M.; Sammarco, M.; Montabone, G.; Tonelli, R.; Deana, M.; Costi, G.; Di Tanno, F.; Prati, M.; et al. Inter-Laboratory Correlation Exercise with Portable Emissions Measurement Systems (PEMS) on Chassis Dynamometers. *Appl. Sci.* **2018**, *8*, 2275. [[CrossRef](#)]

46. Giechaskiel, B.; Casadei, S.; Rossi, T.; Forloni, F.; Di Domenico, A. Measurements of the Emissions of a “Golden” Vehicle at Seven Laboratories with Portable Emission Measurement Systems (PEMS). *Sustainability* **2021**, *13*, 8762. [[CrossRef](#)]
47. Valverde, V.; Giechaskiel, B. Assessment of Gaseous and Particulate Emissions of a Euro 6d-Temp Diesel Vehicle Driven >1300 km Including Six Diesel Particulate Filter Regenerations. *Atmosphere* **2020**, *11*, 645. [[CrossRef](#)]
48. Collins, J.F.; Shepherd, P.; Durbin, T.D.; Lents, J.; Norbeck, J.; Barth, M. Measurements of In-Use Emissions from Modern Vehicles Using an on-Board Measurement System. *Environ. Sci. Technol.* **2007**, *41*, 6554–6561. [[CrossRef](#)] [[PubMed](#)]
49. Seykens, X.; van den Tillaart, E.; Lilova, V.; Nakatani, S. *NH<sub>3</sub> Measurements for Advanced SCR Applications*; SAE Technical Paper 2016-01-0975; SAE: Warrendale, PA, USA.
50. Suarez-Bertoa, R.; Mendoza-Villafuerte, P.; Riccobono, F.; Vojtisek, M.; Pechout, M.; Perujo, A.; Astorga, C. On-Road Measurement of NH<sub>3</sub> Emissions from Gasoline and Diesel Passenger Cars during Real World Driving Conditions. *Atmos. Environ.* **2017**, *166*, 488–497. [[CrossRef](#)]
51. Rahman, M.; Hara, K.; Nakatani, S.; Tanaka, Y. *Development of a Fast Response Nitrogen Compounds Analyzer Using Quantum Cascade Laser for Wide-Range Measurement*; SAE Technical Paper 2011-26-0044; SAE: Warrendale, PA, USA, 2011. [[CrossRef](#)]
52. Suarez-Bertoa, R.; Zardini, A.A.; Lilova, V.; Meyer, D.; Nakatani, S.; Hibel, F.; Ewers, J.; Clairotte, M.; Hill, L.; Astorga, C. Intercomparison of Real-Time Tailpipe Ammonia Measurements from Vehicles Tested over the New World-Harmonized Light-Duty Vehicle Test Cycle (WLTC). *Env. Sci. Pollut. Res.* **2015**, *22*, 7450–7460. [[CrossRef](#)]
53. Li, N.; El-Hamalawi, A.; Barrett, R.; Baxter, J. *Ammonia Measurement Investigation Using Quantum Cascade Laser and Two Different Fourier Transform Infrared Spectroscopy Methods*; SAE Technical Paper 2020-01-0365; SAE: Warrendale, PA, USA, 2020. [[CrossRef](#)]
54. Murtonen, T.; Vesala, H.; Koponen, P.; Pettinen, R.; Kajolinna, T.; Antson, O. *NH<sub>3</sub> Sensor Measurements in Different Engine Applications*; SAE Technical Paper 2018-01-1814; SAE: Warrendale, PA, USA, 2018. [[CrossRef](#)]
55. Wright, N.; Osborne, D.; Music, N. *Comparison of Hydrocarbon Measurement with FTIR and FID in a Dual Fuel Locomotive Engine*; SAE Technical Paper 2016-01-0978; SAE: Warrendale, PA, USA, 2016. [[CrossRef](#)]
56. Suarez-Bertoa, R.; Clairotte, M.; Arlitt, B.; Nakatani, S.; Hill, L.; Winkler, K.; Kaarsberg, C.; Knauf, T.; Zijlmans, R.; Boertien, H.; et al. Intercomparison of Ethanol, Formaldehyde and Acetaldehyde Measurements from a Flex-Fuel Vehicle Exhaust during the WLTC. *Fuel* **2017**, *203*, 330–340. [[CrossRef](#)]
57. Daemme, L.C.; Penteadó, R.; Corrêa, S.M.; Zotin, F.; Errera, M.R. Emissions of Criteria and Non-Criteria Pollutants by a Flex-Fuel Motorcycle. *J. Braz. Chem. Soc.* **2016**, *27*, 2192–2202. [[CrossRef](#)]

**Disclaimer/Publisher’s Note:** The statements, opinions and data contained in all publications are solely those of the individual author(s) and contributor(s) and not of MDPI and/or the editor(s). MDPI and/or the editor(s) disclaim responsibility for any injury to people or property resulting from any ideas, methods, instructions or products referred to in the content.